

Statistical Analysis of the Influence of Interaction Ranges on Structural Phases of Flexible Polymers

Jonathan Gross^a, Thomas Neuhaus^b, Thomas Vogel^a, and Michael Bachmann^a

^aCenter for Simulational Physics, The University of Georgia, Athens, Georgia 30602, USA

^bJülich Supercomputing Centre, Forschungszentrum Jülich, D-52425 Jülich, Germany

Abstract

We investigate the influence of the interaction range of non-bonded monomers in an elastic, flexible polymer upon formation of structural phases. Massively parallel replica-exchange simulations of a generic, coarse-grained polymer model enable the construction of the structural phase diagram by means of microcanonical statistical analysis. Multiple solid phases, a liquid phase, and a gas-like phase can be identified. We find evidence for finite-size effects that cause the crossover of “collapse” and “freezing” transitions for very short interaction ranges.

© 2014 Published by Elsevier B.V. This is an open access article under the CC BY-NC-ND license

(<http://creativecommons.org/licenses/by-nc-nd/3.0/>).

Peer-review under responsibility of The Organizing Committee of CSP 2013 conference

Keywords: Monte Carlo, parallel tempering, phase transitions, polymers, GPU

Introduction and Model

The biological function of proteins is often connected to their three-dimensional geometric structure and misfoldings can be the cause of severe illnesses. Therefore, the study of biopolymers and their dynamical and structural properties is a major topic of interdisciplinary research. Experimental and computational approaches to understand the folding process of proteins and polymers have advanced over the last decades, but many questions still remain unanswered. Even with today’s computing resources all-atom simulations of polymer systems remain a big challenge. Hence, coarse-grained models were developed to capture the essential properties of classes of polymers. Employing a simplified model for flexible, elastic polymers, we recently have investigated how the monomer-monomer interaction range influences structural phases [1]. Although phase transitions only occur in macroscopic systems, local effects, such as the monomer arrangement in the core, competing with surface effects, do play an important role in the nucleation process. That means that macroscopic effects such as condensation, have to pass a series of smaller “subphase” transitions on the microscopic level [2]. These smaller structural transitions do not necessarily scale with the size of the system, see, e.g., Refs. [3–5] for evidence in small atomic clusters and Refs. [6–11] for polymers with finite length. Here, we discuss aspects of the formation of structural phases of flexible polymers by focusing on the range of interaction between the non-bonded monomers. Recent studies of a discrete model [12, 13] indicate that the structure formation is affected by the effective interaction range of non-bonded monomers competing with excluded volume effects. Such insights in the different structural pseudo-phases can only be gained by means of computer simulations. For our study, we applied generalized-ensemble Monte Carlo methods to obtain precise estimates of the density of states, which is the basic quantity for the subsequent microcanonical statistical analysis.

We employ a model for elastic and flexible homopolymers, where the bonds are represented by a finitely extensible nonlinear elastic (FENE) potential [14]

$$U_{\text{FENE}}(r_{ii+1}) = -\frac{K}{2}R^2 \log \left[1 - \left(\frac{r_{ii+1} - r_0}{R} \right)^2 \right]. \quad (1)$$

In addition, the shifted and truncated Lennard-Jones potential

$$U_{\text{LJ}}^{\text{mod}}(r_{ij}) = U_{\text{LJ}}(r_{ij}) - U_{\text{LJ}}(r_c) \quad (2)$$

describes the interaction between all monomers. It carries an additional parameter r_s to adjust the effective width of the potential:

$$U_{\text{LJ}}(r_{ij}) = 4\epsilon \left[\left(\frac{\sigma}{r_{ij} - r_s} \right)^{12} - \left(\frac{\sigma}{r_{ij} - r_s} \right)^6 \right]. \quad (3)$$

The total energy of a conformation $C = (\vec{r}_1, \dots, \vec{r}_N)$ for an N -mer is given by

$$E(C) = \sum_{i < j}^N U_{\text{LJ}}^{\text{mod}}(r_{ij}) + \sum_i^{N-1} U_{\text{FENE}}(r_{ii+1}). \quad (4)$$

Details of the parametrization are given in Ref. [1]. We introduce a parameter δ to define the width of the Lennard-Jones potential, such that $\delta = r_2 - r_1 = \lambda(r_0 - r_s)$, where r_1 and r_2 are the two radii where $U_{\text{LJ}}^{\text{mod}}(r_1) = U_{\text{LJ}}^{\text{mod}}(r_2) = -\epsilon_{\text{sq}} = -(0.5\epsilon + U_{\text{LJ}}(r_c))$, see Fig. 1. The maximum value of δ is determined by the unmodified Lennard-Jones potential,

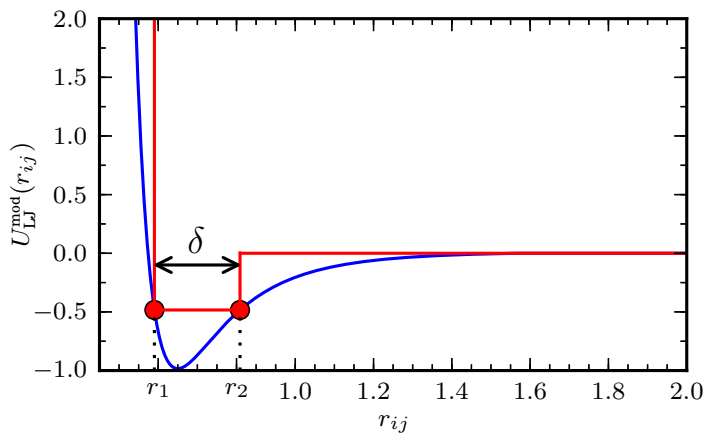


Figure 1: (Color online) The potential width δ is defined by the width of a square well potential of depth $-\epsilon_{\text{sq}}$; it is the difference of the two distances r_1 and r_2 , where the Lennard-Jones potential equals $-\epsilon_{\text{sq}}$.

i.e., at $r_s = 0$, and it is found to be $\delta_{\text{max}} = \lambda r_0 \approx 0.218667$ with $\lambda \approx 0.312382$ [1]. The simulations were carried out by employing the replica-exchange Monte Carlo algorithm, better known as parallel-tempering [15–17]. In this method, n copies of the system are simulated at different temperatures. Each replica of the polymer is updated by proposing a random local displacement of one monomer. This proposal is accepted with the probability given by the Metropolis criterion [18]: $p = \min(1, \exp[-\beta(E_{\text{new}} - E_{\text{old}})])$, where $\beta = 1/k_B T$ is the inverse thermal energy, and E_{old} and E_{new} are the energies of the conformations before and after the proposal. After a fixed number of independent Metropolis updates of each replica has been performed, an exchange between neighboring copies i and j with inverse temperatures β_i and β_j , respectively, is suggested. The probability of accepting the replica exchange is $p = \min(1, \exp[(E_i - E_j)(\beta_i - \beta_j)])$. This procedure enables each copy of the system to heat up and cool down over the whole simulated temperature interval and introduces a global update to the system. The replica-exchange algorithm is pleasingly parallel and can be efficiently implemented on massively parallel hardware such as graphics processing units (GPUs). In addition, we parallelized the energy calculation of the pairwise potentials, necessary at each Monte Carlo step. The benefits of this approach are discussed in detail in Ref. [19].

For very short interaction ranges, the first-order character of the freezing transition becomes so distinct that another algorithmic improvement becomes necessary. Simulating multiple Gaussian modified ensembles (MGME) [20]

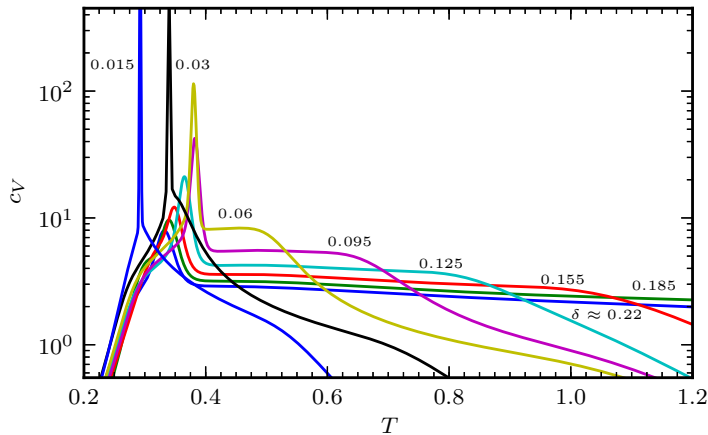


Figure 2: (Color online) Specific heats for the 90-mer for seven values of δ .

enables us to sample entropically suppressed conformations in the phase coexistence transition region. The principal idea of MGME is to flatten all bimodal Boltzmann probability distributions by multiplying these by appropriate Gaussian forms. Thus, with a Gaussian form centered around the minimum energy $E_{G,i}$ in the well between the peaks of the canonical distribution in the i -th ensemble, the probability for a state with energy E in the modified ensemble becomes $P_{\text{MGME},i}(E) \sim \exp(S(E) - \beta_i E - [(E - E_{G,i})/(\Delta E_G)]^2)$. The Gaussian form is a counter-term to $S(E) = \ln g(E)$ the microcanonical entropy, with $g(E)$ being the density of states, see [1, 20] for details.

Results

The goal of our investigation is to derive a structural phase diagram parametrized by the potential width δ and temperature T . Typically, one analyzes the peak position of thermodynamic quantities like the specific heat or the thermal fluctuations of geometrical parameters like the radius of gyration. For the simulated 90-mer the specific heat curves for seven exemplary potential widths δ are shown in Fig. 2. With decreasing interaction range we see large shifts of the “collapse” transition, to lower temperatures, characterized by the shoulders in the plots. The freezing transition, signaled by the pronounced peak at lower temperatures, shifts to slightly higher temperature as we lower the potential width. For very narrow potentials the freezing temperature becomes lower again. The maximum values of those peaks, however, increase proportionally with δ over the whole range, indicating that the freezing transitions becomes stronger. While, in principle it is possible to identify all transition points by looking at canonical quantities such as the specific heat, some transitions are difficult to locate and one has to refer to different quantities to uncover the precise location of a transition.

An alternative way of identifying conformational transitions is a thorough analysis of the density of states and its derivatives [8, 21–23]. All information about the system is encoded into the density of states, including phase or structural transitions. Some transitions, such as the solid-solid transition, can be identified much easier by microcanonical analysis [9, 13, 21]. We convinced ourselves that both approaches yield the same qualitative answers. The phase diagram of a 90-mer, as shown in Fig. 3, is constructed using microcanonical analysis, and it is parametrized by the interaction range δ and the temperature T . At high temperatures and short interaction ranges, in the “gas” phase **G**, the polymers most likely will form extended coils. Lowering the temperature in the gas phase, we approach the Θ -transition, marked by the line with the symbol \times in the phase diagram. The expanded polymer coils collapse into globular structures that have no crystalline internal structure. This “liquid”-phase **L** only appears for interaction ranges $\delta \gtrsim 0.02$. The freezing transition is marked by the line with + symbols. The “liquid” polymer crystallizes at low temperatures. For very short attraction range, we see a direct transition from gas to solid, as the temperature interval of the liquid phase gets smaller and smaller with decreasing potential width. Microcanonically, we observe a crossover of the transition temperature for collapse and freezing transition, as shown in the inset of Fig. 3. We

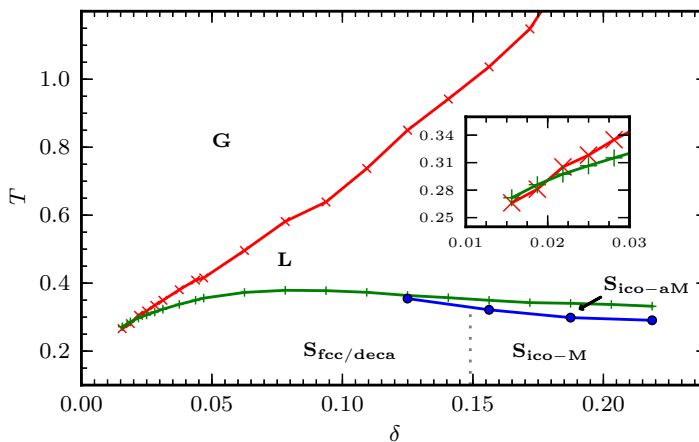


Figure 3: (Color online) Phase diagram for the 90-mer, obtained by microcanonical analysis. The inset shows the crossover of the transition temperatures for collapse and freezing transition.

identify multiple solid phases below the freezing transition line. For the unmodified Lennard-Jones potential, i.e., for $\delta = \delta_{\max}$, and values $\delta \gtrsim 0.12$, we find two icosahedral-like solid structures. $S_{\text{ico-aM}}$ is a solid phase with one or more icosahedral cores and an incomplete anti-Mackay like (hcp) outer shell. Reducing the temperature further, we cross the solid-solid transition line, where the crystalline structure is changed into Mackay-type fcc layers, i.e., in phase $S_{\text{ico-M}}$, (cp. Ref. [7]). For interaction ranges below $\delta \approx 0.15$, the icosahedral core is energetically less favorable over the decahedral packaging of monomers that now dominates the solid phase $S_{\text{fcc/deca}}$. This behavior has already been observed in atomic cluster models earlier [3–5]. A systematic analysis of the properties of solid polymer phases has been performed in Ref. [1] for the exemplified 55-mer. The 55-mer is known to form a perfect icosahedron with a Mackay-like overlayer for $\delta = \delta_{\max}$. It exhibits a transition from icosahedral to fcc via decahedral intermediate structures, see Refs. [1, 4].

Summary

We have investigated the influence of the potential width of non-bonded monomer-monomer interaction on the structure formation of flexible polymers by means of replica-exchange Monte Carlo simulations. We constructed the structural phase-diagram for classes of flexible, elastic polymers with 90 monomers, parametrized by temperature and interaction range. This was achieved by both, canonical and microcanonical statistical analysis. A “gas”-phase, a “liquid”-phase, and multiple solid phases as well as the transitions between these phases were identified. Similar to atomic clusters, the polymer crystals undergo transitions from icosahedral to decahedral and fcc structures with decreasing potential widths.

Acknowledgments

This work has been partially supported by the NSF under Grant No. DMR–1207437 and by the supercomputer time grant VSR Project 5082 of the Forschungszentrum Jülich.

References

- [1] J. Gross, T. Neuhaus, T. Vogel, and M. Bachmann, *J. Chem. Phys.* **138**, 074905 (2013).
- [2] C. Junghans, M. Bachmann, and W. Janke, *Phys. Rev. Lett.* **97**, 218103 (2006); C. Junghans, W. Janke, and M. Bachmann, *Comp. Phys. Commun.* **182**, 1937 (2011).
- [3] J. P. K. Doye, D. J. Wales, and R. S. Berry, *J. Chem. Phys.* **103**, 4234 (1995).
- [4] J. P. K. Doye and D. J. Wales, *J. Phys. B.: At. Mol. Opt. Phys.* **29**, 4589 (1996).

- [5] L. Cheng and J. Yang, J. Phys. Chem. A **111**, 5287 (2007).
- [6] T. Vogel, M. Bachmann, and W. Janke, Phys. Rev. E **76**, 061803 (2007).
- [7] S. Schnabel, T. Vogel, M. Bachmann, and W. Janke, Chem. Phys. Lett. **476**, 201 (2009); S. Schnabel, M. Bachmann, and W. Janke, J. Chem. Phys. **131**, 124904 (2009).
- [8] D. T. Seaton, T. Wüst, and D. P. Landau, Comp. Phys. Comm. **180**, 587 (2009); Phys. Rev. E **81**, 011802 (2010).
- [9] S. Schnabel, D. T. Seaton, D. P. Landau, and M. Bachmann, Phys. Rev. E **84**, 011127 (2011).
- [10] T. Vogel, T. Neuhaus, M. Bachmann, and W. Janke, Europhys. Lett. **85**, 10003 (2009).
- [11] T. Vogel, T. Neuhaus, M. Bachmann, and W. Janke, Phys. Rev. E **80**, 011802 (2009).
- [12] F. Rampf, W. Paul, and K. Binder, Europhys. Lett. **70**, 628 (2005); W. Paul, T. Strauch, F. Rampf, and K. Binder, Phys. Rev. E **75**, 060801(R) (2007).
- [13] M. P. Taylor, W. Paul, and K. Binder, J. Chem. Phys. **131**, 114907 (2009); Phys. Rev. E **79**, 050801(R) (2009).
- [14] R. B. Bird, C. F. Curtiss, R. C. Armstrong, and O. Hassager, *Dynamics of Polymeric Liquids*, Second Edition, (Wiley, New York, 1987).
- [15] R. H. Swendsen and J.-S. Wang, Phys. Rev. Lett. **57**, 2607 (1986).
- [16] C. J. Geyer, in *Computing Science and Statistics: Proceedings of the 23rd Symposium on the Interface*, E. M. Keramidas (editor), p. 156–163 (Interface Foundation, Fairfax, Virginia, 1991).
- [17] K. Hukushima and K. Nemoto, J. Phys. Soc. Jpn. **65**, 1604 (1996).
- [18] N. Metropolis, A. W. Rosenbluth, M. N. Rosenbluth, A. H. Teller, and E. Teller, J. Chem. Phys. **21**, 1087 (1953).
- [19] J. Gross, W. Janke, and M. Bachmann, Comput. Phys. Commun. **182**, 1638 (2011); Phys. Proc. **15**, 29 (2011).
- [20] T. Neuhaus and J. S. Hager, Phys. Rev. E **74**, 036702 (2006).
- [21] D. H. E. Gross, *Microcanonical Thermodynamics* (World Scientific, Singapore, 2001).
- [22] M. Möddel, M. Bachmann, and W. Janke, Macromolecules **44**, 9013 (2011).
- [23] W. Janke, Nucl. Phys. B. **63A–C**, 631 (1998).